Model-Independent Source Imaging Using Two-Pion Correlations in (2 to 8)*A* GeV Au+Au Collisions

S. Y. Panitkin,[7] N. N. Ajitanand,[12] J. Alexander,[12] M. Anderson,[5] D. Best,[1] F. P. Brady,[5] T. Case,[1] W. Caskey,[5] D. Cebra,[5] J. Chance,[5] P. Chung,[12] B. Cole,[4] K. Crowe,[1] A. Das,[10] J. Draper,[5] M. Gilkes,[11] S. Gushue,[2] M. Heffner,[5] A. Hirsch,[11] E. Hjort,[11] L. Huo,[6] M. Justice,[7] M. Kaplan,[3] D. Keane,[7] J. Kintner,[8] J. Klay,[5] D. Krofcheck,[9] R. Lacey,[12] J. Lauret,[12] M. A. Lisa,[10] H. Liu,[7] Y. M. Liu,[6] R. McGrath,[12] Z. Milosevich,[3] G. Odyniec,[1] D. Olson,[1] C. Pinkenburg,[12] N. Porile,[11] G. Rai,[1] H. G. Ritter,[1] J. Romero,[5] R. Scharenberg,[11] L. S. Schroeder,[1] B. Srivastava,[11] N. T. B. Stone,[2] T. J. M. Symons,[1] S. Wang,[7] R. Wells,[10] J. Whitfield,[3] T. Wienold,[1] R. Witt,[7] L. Wood,[5] X. Yang,[4] W. N. Zhang,[6] and Y. Zhang[4]

(E895 Collaboration)

D. A. Brown[13] and P. Danielewicz[14]

[1]*Lawrence Berkeley National Laboratory, Berkeley, California 94720*
[2]*Brookhaven National Laboratory, Upton, New York 11973*
[3]*Carnegie Mellon University, Pittsburgh, Pennsylvania 15213*
[4]*Columbia University, New York, New York 10027*
[5]*University of California, Davis, California 95616*
[6]*Harbin Institute of Technology, Harbin 150001, People's Republic of China*
[7]*Kent State University, Kent, Ohio 44242*
[8]*St. Mary's College of California, Moraga, California 94575*
[9]*University of Auckland, Auckland, New Zealand*
[10]*The Ohio State University, Columbus, Ohio 43210*
[11]*Purdue University, West Lafayette, Indiana 47907*
[12]*State University of New York, Stony Brook, New York 11794*
[13]*University of Washington, Seattle, Washington 98195*
[14]*Michigan State University, East Lansing, Michigan 48824*

(Received 9 June 2000; published 24 August 2001)

We report a particle source imaging analysis based on two-pion correlations in high multiplicity Au+Au collisions at beam energies between 2*A* and 8*A* GeV. We apply the imaging technique introduced by Brown and Danielewicz, which allows a model-independent extraction of source functions with useful accuracy out to relative pion separations of about 20 fm. The extracted source functions have Gaussian shapes. Values of source functions at zero separation are almost constant across the energy range under study. Imaging results are found to be consistent with conventional source parameters obtained from a multidimensional Hanburg-Brown–Twiss analysis.

DOI: 10.1103/PhysRevLett.87.112304 PACS numbers: 25.75.Gz

One of the robust predictions of quantum chromodynamics is that strongly interacting matter can exist in a state with colored degrees of freedom, i.e., quarks and gluons, if subjected to sufficiently high temperature or density [1]. This deconfined state of matter, often called quark-gluon plasma (QGP), may have been present in the Universe a few μs after the big bang. It is also believed that QGP can be produced in collisions of heavy ions at high energies. Experimental searches for evidence of QGP are prominent and challenging priorities in modern heavy-ion physics. A major difficulty is that the soughtafter QGP is a transient state which persists only for time scales on the order of fm/c. After expansion and cooling, any QGP necessarily undergoes a phase transition to hadronic matter, possibly leaving little evidence behind in the final state of the collision. Numerous experimental observables have been proposed as signatures of QGP creation in heavy-ion collisions [2]. One of the more promising of these is based on the expectation that the larger number of degrees of freedom associated with the deconfined state should manifest itself in increased system entropy, which ought to survive subsequent hadronization and freeze out. The specific prediction is that QGP formation will cause the system to expand more and/or interact for a longer time and produce more particles, relative to a system which remained in the hadronic phase throughout the collision process.

Intensity interferometry [3] has been extensively used to extract information about spatial-temporal properties of heavy-ion collisions. The HBT approach [3–8] is well understood from the theoretical point of view, and is the mainstream analysis method for meson (π, K) intensity interferometry. Meson final-state interactions are simple, so one may remove most of the distortion of the final-state wave functions with a simple Coulomb correction. Furthermore, in the traditional analysis one does not ask for more than the widths of the underlying source function. A novel approach—the imaging technique introduced by Brown and Danielewicz [9–11]—offers the opportunity

to use *any* class of like-pair correlations to reconstruct the entire source function, as opposed to the conventional model-dependent parametrization. The two approaches have natural connections, which are especially clear for the case of noninteracting spin-zero bosons [12]. In this paper, we report the first application of the source imaging technique to experimental data, specifically negative pions from Au+Au collisions at beam energies between 2*A* and 8*A* GeV, with particular emphasis on verification and study of the expected connection with the source parameters obtained from HBT analysis. Comparing the two methods not only allows us to test the model underlying the HBT parametrization, but also lends credibility to the source imaging approach in other contexts such as proton-proton correlations.

We present data from experiment E895 [13], in which Au beams of kinetic energy 1.85*A*, 3.9*A*, 5.9*A*, and 7.9*A* GeV from the Alternating Gradient Synchrotron (AGS) accelerator at Brookhaven were incident on a fixed Au target. The analyzed π^- samples come from the main E895 subsystem—the EOS time projection chamber (TPC) [14], located in a dipole magnetic field of 0.75 or 1.0 T. Results of the E895 π^- HBT analysis were reported earlier [15], and in this Letter, we focus on an application of imaging to the same datasets.

In order to obtain the two-pion correlation function C_2 experimentally, the standard event-mixing technique was used [16]. Negative pions were detected and reconstructed over a substantial fraction of 4π solid angle in the center-of-mass frame, and simultaneous measurement of particle momentum and specific ionization in the TPC gas helped to separate π^- from other negatively charge particles, such as electrons, K^-, and antiprotons. Contamination from these species is estimated to be under 5%, and is even less at the lower beam energies and higher transverse momenta. Momentum resolution in the region of correlation measurements is better than 3%. Event centrality selection was based on the multiplicity of reconstructed charged particles. In the present analysis, events were selected with a multiplicity corresponding to the upper 11% of the inelastic cross section for Au+Au collisions. Only pions with p_T between 100 and 300 MeV/c and within ± 0.35 units from midrapidity were used. Another requirement was for each used π^- track to point back to the primary event vertex with a distance of closest approach (DCA) less than 2.5 cm. This cut removes most pions originating from weak decays of long-lived particles, e.g., Λ and K^0. Monte Carlo simulations based on the relativistic quantum molecular dynamics (RQMD) model [17] indicate that decay daughters are present at a level that varies from 5% at 4*A* GeV to 10% at 8*A* GeV, and they lie preferentially at $p_T < 100$ MeV/c. Finally, in order to overcome effects of track merging, a cut on spatial separation of two tracks was imposed. For pairs from both "true" and "background" distributions, the separation between two tracks was required to be greater than 4.5 cm over a distance of 18 cm in the beam direction. This cut also suppresses effects of track splitting [15]. Besides such cuts, the correlation functions themselves were corrected for Coulomb final-state interactions and finite momentum resolution effects, using an iterative technique similar to that used by the NA44 Collaboration [18]. See [15] for details. Note, that this procedure does not impose a Gaussian shape on a non-Gaussian correlation function.

Imaging [9,10] was used to extract the shape of the source from the measured correlation functions. It has been shown [11] that imaging allows robust reconstruction of the source function for systems with nonzero lifetime, even in the presence of strong space-momentum correlations. The main features of the method are outlined below; see Refs. [9,10,12] for more details. The full two-particle correlation function may be expressed as

$$C_{\mathbf{P}}(\mathbf{Q}) - 1 = \int d\mathbf{r}\, K(\mathbf{Q},\mathbf{r}) S_{\mathbf{P}}(\mathbf{r}), \qquad (1)$$

where $K = |\Phi_{\mathbf{Q}}^{(-)}(\mathbf{r})|^2 - 1$, the total momentum of the pair is $\mathbf{P}$, the relative momentum is $\mathbf{Q} = \mathbf{p}_1 - \mathbf{p}_2$, and the relative separation of emission points is $\mathbf{r}$. Both $\mathbf{r}$ and $\mathbf{Q}$ are written in the pair center of mass frame. Here, $\Phi_{\mathbf{Q}}^{(-)}$ is the relative wave function of the pair and for spin-0 bosons in the absence of final-state interactions, it is the symmetrized sum of free waves:

$$\Phi_{\mathbf{Q}}^{(-)}(\mathbf{r}) = \frac{1}{\sqrt{2}} (e^{i\mathbf{Q}/2\cdot\mathbf{r}} + e^{-i\mathbf{Q}/2\mathbf{r}}). \qquad (2)$$

However, in general it may be quite complicated. The goal of imaging is to determine the relative source function [$S_{\mathbf{P}}(\mathbf{r})$ in Eq. (1)], given $C_{\mathbf{P}}(\mathbf{Q})$. The problem of imaging then becomes the problem of inverting $K(\mathbf{Q},\mathbf{r})$. The source function, $S_{\mathbf{P}}(\mathbf{r})$, is the distribution of relative separations of emission points for the two particles in their center-of-mass frame. For an expanding source, $S_{\mathbf{P}}(\mathbf{r})$ corresponds to the region of homogeneity, the region from where particle pairs with a given mean momentum P are emitted, and this region is smaller than the whole (momentum-integrated) source in coordinate space. In this Letter, we analyze the pion correlations in Q_{inv}. The transition from the full three-dimensional problem in Eq. (1) to the angle-averaged problem is straightforward: one expands the source and correlation in spherical harmonics [9] and keeps $\ell = m = 0$ terms. The angle-averaged version of Eq. (1) is

$$C(Q_{\text{inv}}) - 1 = 4\pi \int dr\, r^2 K(Q_{\text{inv}}, r) S(r). \qquad (3)$$

Here $Q_{\text{inv}} = \sqrt{\mathrm{Q}^2 - Q_0^2}$ and since $Q_0 = 0$ in the pair CM frame, $Q_{\text{inv}} = |\mathbf{Q}|$. Thus, while the source one reconstructs is a distribution in the pair CM frame, the inversion itself may be done with correlations constructed in any frame. In this equation, the kernel is simply averaged over the angle between $\mathbf{Q}$ and $\mathbf{r}$:

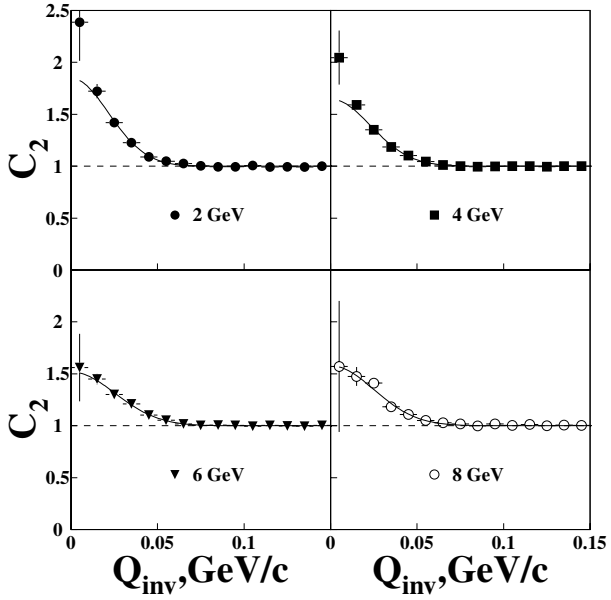

FIG. 1. Measured two-pion correlation functions for Au+Au central collisions at four beam energies. Lines represent Gaussian fits to the data

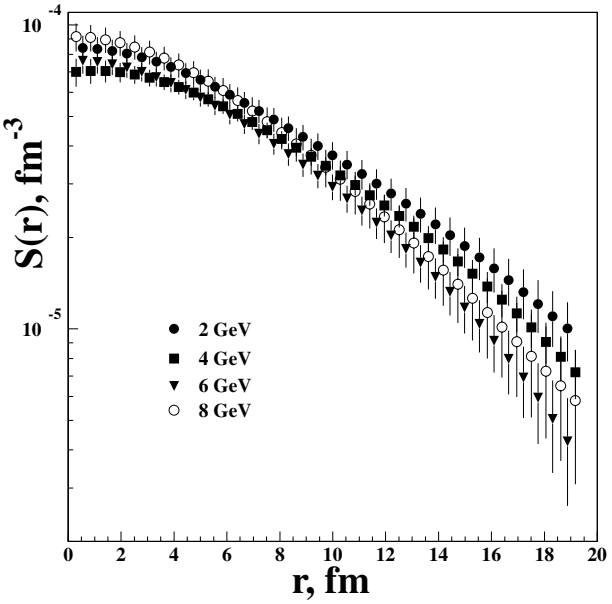

FIG. 2. Relative source functions extracted from the pion correlation data at 2*A*, 4*A*, 6*A*, and 8*A* GeV.

$$K(Q_{\rm inv}, r) = \frac{1}{2}\int_{-1}^{1}(\cos\theta_{\mathbf{Qr}})K(\mathbf{Q},\mathbf{r})\,. \quad (4)$$

For identical spin-zero bosons with no FSI, this kernel is

$$K(Q_{\rm inv}, r) = \sin(Q_{\rm inv}r)/Q_{\rm inv}r\,. \quad (5)$$

We comment that since the $\mathbf{r} = 0$ point of the source is a maximum, it is spherically symmetric in a neighborhood around that point and $S(r \to 0) = S(\mathbf{r} \to 0)$.

We now proceed as in [19] and expand the radial dependence of the source in a basis spline basis: $S(r) = \sum_j S_j B_j(r)$. With this, Eq. (1) becomes a matrix equation $C_i = \sum_j K_{ij} S_j$ with a new kernel:

$$K_{ij} = \int dr\, K(Q_i, r) B_j(r)\,. \quad (6)$$

Here, and for the rest of the paper, we have dropped the "inv" subscript on Q. Imaging reduces to finding the set of source coefficients, S_j, that minimize the χ^2. Here, $\chi^2 = \sum_i (C_i - \sum_j K_{ij} S_j)^2/\Delta^2 C_i$. This set of source coefficients is $S_j = \sum_i [(K^T(\Delta^2 C)^{-1}K)^{-1}K^T B]_{ji}(C_i - 1)$, where K^T is the transpose of the kernel matrix. The uncertainty of the source coefficients is the square root of the diagonal elements of the covariance matrix of the source, $\Delta^2 S = [K^T(\Delta^2 C)^{-1}K]^{-1}$. The uncertainty on $S(r)$ itself is given by $\Delta S(r) = \sqrt{\sum_{i,j=1}^{N_M} \Delta^2 S_{ij} B_i(r) B_j(r)}$.

For the case of noninteracting spin-zero bosons with Gaussian correlations, there is a natural connection between the imaged sources and "standard" HBT parameters [12]—the source is a Gaussian with the "standard" HBT parameters as radii:

$$S(\mathbf{r}) = \frac{\lambda}{(2\sqrt{\pi})^3\sqrt{\det[R^2]}}\exp\left(-\frac{1}{4}\, r_i r_j [R^2]^{-1}_{ij}\right). \quad (7)$$

Here λ is a fit parameter traditionally called the chaoticity or coherence factor in HBT analyses and $[R^2]$ is the real symmetric matrix of radius parameters

$$[R^2] = \begin{pmatrix} R_o^2 & R_{os}^2 & R_{o\ell}^2 \\ R_{os}^2 & R_s^2 & R_{s\ell}^2 \\ R_{o\ell}^2 & R_{s\ell}^2 & R_\ell^2 \end{pmatrix}. \quad (8)$$

A possible interpretation of λ parameter is that it measures the fraction of the particles emitted from the core of the interactions as compared to the particles emitted from the unresolved (very extended, $\geq$20 fm) halo of long-lived resonances such as η, η' [20]. Equation (7) is the most general Gaussian one may use, but usually one assumes a cylindrical symmetry of the single particle source so that there is only one nonvanishing nondiagonal element R_{ol}^2. The asymptotic value of the relative source function at zero separation $S(\mathbf{r} \to 0)$ is related to the inverse effective volume of particle emission, and has units of fm^{-3}:

$$S(\mathbf{r} \to 0) = \frac{\lambda}{(2\sqrt{\pi})^3\sqrt{\det[R^2]}}. \quad (9)$$

TABLE I. Radius parameters of Gaussian fits to the extracted source (R_S) functions and measured correlation functions (R_{C2}) for different energies.

E_b (A GeV)	2	4	6	8
R_S (fm)	6.70 ± 0.04	6.35 ± 0.03	5.56 ± 0.03	5.53 ± 0.05
R_{C2} (fm)	6.39 ± 0.2	6.05 ± 0.1	5.51 ± 0.15	5.61 ± 0.28

As it was shown in [12] $S(\mathbf{r} \to 0)$ is an important parameter needed to extract the space-averaged phase-space density. Figure 1 shows measured angle-averaged two-pion correlation functions for central Au+Au collisions at 2A, 4A, 6A, and 8A GeV. Figure 2 shows relative source functions $S(r)$ obtained by applying the imaging technique to the measured two-pion correlation functions. Note that the plotted points are for representation of the continuous source function and hence are not statistically independent of each other as the source functions are expanded in basis splines [19]. Since the source covariance matrix is not diagonal, the coefficients of the basis spline expansion are also not independent, which is taken into account during χ^2 calculations. The sources shown in Fig. 2 are consistent with zero, within errors, in the region past $\approx$20 fm. Thus with this technique, we may reconstruct the distribution of relative pion separations with useful accuracy out to $r \sim 20$ fm.

The images obtained at each of the four E895 beam energies are rather similar in shape, and upon fitting with a Gaussian function, values of χ^2 per degree of freedom between 0.9 and 1.2 are obtained. Results of fits to the source function and correlation functions are shown in Table I. One can see that source radii extracted via both techniques are similar, further confirming the validity of a Gaussian source hypothesis. Indeed, the somewhat smaller errors on the R_S parameters compared to R_{C2} are consistent with the Gaussian fit function being in closer overall agreement with the data points in the case of the imaging approach.

Figure 3 compares the effective volumes of pion emission inferred from the standard Bertsch-Pratt pion HBT parametrization (open circles) with the effective volumes derived from the image source functions shown in Fig. 2 (solid circles), recalling that $S(\mathbf{r} \to 0) = S(r \to 0)$. Essentially, this figure plots the inverse of the left- and right-hand sides of Eq. (9). It can be seen from Fig. 3 that the agreement between imaging and the HBT parametrization is fairly good. Values of source functions at zero separation as well as HBT source size parameters (published in Ref. [15] and reproduced in Table II) are approximately constant within errors across the 2A to 8A GeV beam energy range.

In summary, we present measurements of one-dimensional correlation functions for negative pions emitted at midrapidity from central Au+Au collisions at 2A, 4A, 6A, and 8A GeV. These correlation functions are analyzed using the imaging technique of Brown and Danielewicz. It is found that relative source functions $S(r)$ have rather similar shapes, while zero-separation intercepts $S(r \to 0)$, which are related to the effective volume of pion emission, are almost constant across the range of bombarding energies under study. Distributions of relative separation have been measured out to 20 fm, and the extracted source functions are approximately Gaussian. We have performed the first experimental check of the predicted connection between imaging and traditional meson interferometry techniques and found that the two methods are in good agreement. Overall, results of this investigation strengthen the rationale for applying systematic imaging analyses to a variety of particle species (i.e., strongly interacting particles such as protons, antiprotons, etc., as well as pions), and open the door to more detailed inferences about spacetime structure. Such inferences can play an important role in resolving outstanding questions about deconfined nuclear matter.

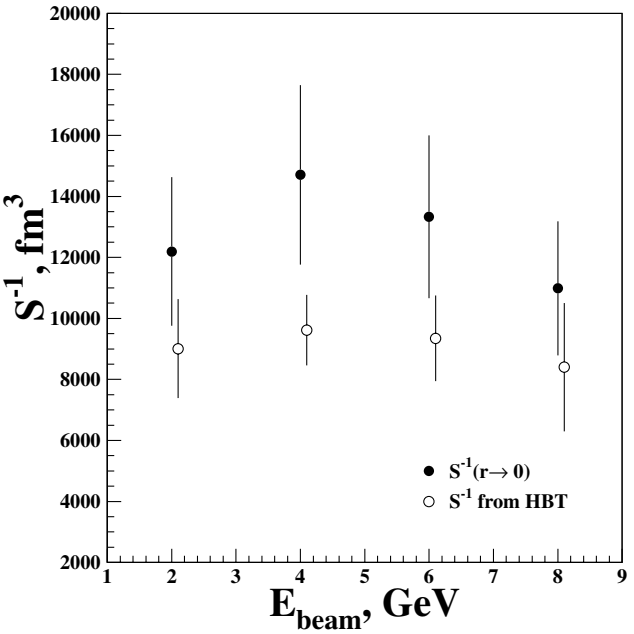

FIG. 3. Values of inverse relative source functions at zero separation as a function of beam energy, obtained using imaging (solid circles) and HBT (open circles).

TABLE II. Fit parameters for the Bertsch-Pratt HBT parametrization of the pion correlation functions for E895 beam energies used for evaluation of $S(r \to 0)$.

E_b (A GeV)	2	4	6	8
λ	0.99 ± 0.06	0.74 ± 0.03	0.65 ± 0.03	0.65 ± 0.05
R_o (fm)	6.22 ± 0.26	5.79 ± 0.16	5.76 ± 0.23	5.49 ± 0.31
R_s (fm)	6.28 ± 0.20	5.37 ± 0.11	5.05 ± 0.12	4.83 ± 0.21
R_l (fm)	5.15 ± 0.19	5.15 ± 0.14	4.72 ± 0.18	4.64 ± 0.24
R_{ol}^2 (fm)	−2.43 ± 1.71	0.43 ± 1.03	2.17 ± 1.20	−0.65 ± 1.85

Stimulating discussions with Dr. G. F. Bertsch, Dr. S. Pratt, Dr. S. A. Voloshin, and Dr. N. Xu are gratefully acknowledged. This research is supported by US DOE, NSF, and other funding, as detailed in Ref. [21].

[1] E. V. Shuryak, Phys. Rep. **61**, 71 (1980).
[2] B. Müller, Nucl. Phys. **A661**, 272 (1999).
[3] V. G. Grishin, G. I. Kopylov, and M. I. Podgoretski, Sov. J. Nucl. Phys. **13**, 638 (1971).
[4] S. Pratt, T. Csörgö, and T. Zimányi, Phys. Rev. C **42**, 2646 (1990).
[5] C. Gelbke and B. K. Jennings, Rev. Mod. Phys. **62**, 553 (1990).
[6] S. Pratt, Nucl. Phys. **A638**, 125c (1998).
[7] U. A. Wiedemann and U. Heinz, Phys. Rep. **319**, 145 (1999).
[8] U. Heinz and B. Jacak, Annu. Rev. Nucl. Part. Sci. **49**, 529 (1999).
[9] D. A. Brown and P. Danielewicz, Phys. Lett. B **398**, 252 (1997).
[10] D. A. Brown and P. Danielewicz, Phys. Rev. C **57**, 2474 (1998).
[11] S. Y. Panitkin and D. A. Brown, Phys. Rev. C **61**, 021901 (2000).
[12] D. A. Brown, S. Y. Panitkin, and G. F. Bertsch, Phys. Rev. C **62**, 014 904 (2000.
[13] G. Rai *et al.,* proposal LBL-PUB-5399, 1993.
[14] G. Rai *et al.,* IEEE Trans. Nucl. Sci. **37**, 56 (1990).
[15] E895 Collaboration, M. A. Lisa *et al.,* Phys. Rev. Lett. **84**, 2798 (2000).
[16] G. Kopylov, Phys. Lett. **50B**, 472 (1974).
[17] H. Sorge, Phys. Rev. C **52**, 3291 (1995).
[18] H. Boggild *et al.,* Phys. Lett. B **302**, 510 (1993).
[19] D. A. Brown and P. Danielewicz, Phys. Rev. C **64**, 014902 (2001); C. de Boor, *A Practical Guide to Splines* (Springer-Verlag, New York, 1978).
[20] T. Csorgo, B. Lorstad, and J. Zimanyi, Z. Phys. C **71**, 491-497 (1996).
[21] E895 Collaboration, P. Chung *et al.,* Phys. Rev. Lett. **85**, 940 (2000).